Electrically driven terahertz radiation of 2DEG plasmons in AlGaN/GaN structures at 110 K temperature

V. Jakštas,[1] I. Grigelionis,[1] V. Janonis,[1] G. Valušis,[1] I. Kašalynas,[1,a)] G. Seniutinas,[2,3] S. Juodkazis,[2,3] P. Prystawko,[4] and M. Leszczyński[4]
[1]*Center for Physical Sciences and Technology, Saulėtekio al. 3, LT-10222 Vilnius, Lithuania*
[2]*Swinburne University of Technology, John St. Mail H34, Hawthorn, VIC 3122, Australia*
[3]*Melbourne Centre for Nanofabrication, ANFF, 151 Wellington Road, Clayton, VIC 3168, Australia*
[4]*Institute of High Pressure Physics UNIPRESS, Sokołowska 29/37, 01-142 Warsaw, Poland*

(Received 6 January 2017; accepted 28 April 2017; published online 15 May 2017)

We experimentally observed a terahertz (THz) radiation of electrically driven 2D electron gas (2DEG) plasmons in AlGaN/AlN/GaN structures at T = 110 K. The grating with a period of 1.0 μm and a filling factor of 0.35 was used to couple electromagnetic radiation out from the plasmonic sample excited in a pulsed regime. The peak power radiated from ungated 2DEG plasmons at a frequency of 5.0 THz under an electric field of 450 V/cm was up to 940 nW. The intensity of the radiation was sufficient to measure spectra with a conventional far-infrared Fourier transform spectrometer. The analysis of the data revealed that the 2DEG plasmon radiation was superimposed with the black-body radiation of the sample and electroluminescence of the impurities. The strategy to reach higher powers of THz emission for practical applications is discussed. *Published by AIP Publishing*. [http://dx.doi.org/10.1063/1.4983286]

The demand for compact and spectrally tunable terahertz (THz) sources motivates scientific community to explore solutions using plasma wave electronics for a couple of decades.[1,2] The first observation of 2D electron gas (2DEG) plasma oscillations in a Si metal-oxide-semiconductor field-effect transistor (Si-MOS-FET)[1] triggered a search of electron plasma instabilities in a different class of material systems such as AlGaAs/GaAs and AlGaN/GaN.[3,4] The developed theory of plasma wave electronics proposed tunable solid-state THz sources driven by a dc-current flow in a lateral plane of the FET channel.[5] However, the intensity of THz plasmon radiation appeared to be not sufficient for practical applications due to the limited coupling efficiency of 2DEG plasmons to the radiative modes.[6–9]

All attempts to demonstrate electrically driven plasmon emission spectra have been limited to low cryogenic temperatures of 10 K or lower.[10,11] Far-infrared emission spectroscopy of 2DEG plasmons in the AlGaAs/GaAs heterojunction revealed the plasmon emission lines in the THz range with the emission frequency inversely proportional to the period of the grating couplers used.[11] More recently, 2DEG plasmons in the GaAs/AlGaAs system were demonstrated tracing the gated and ungated 2DEG plasmon dispersion in time and frequency domains via modified THz time domain spectroscopy.[2] Also, the same materials' structures allowed an experimental observation of a coherent coupling between the localized plasmonic excitations and formation of an one-dimensional THz plasmonic crystal in a strongly modulated 2DEG.[10,12]

The wide-bandgap AlGaN/GaN materials facilitate the plasmonic resonances to appear at higher frequencies due to the available larger charge density in comparison to the AlGaAs/GaAs system.[13,14] The grating-gated AlGaN/GaN structures have demonstrated strong plasmon absorption modes tunable by the electric field and persistent in the spectrum at relatively high temperatures up to 170 K.[4] Independently, an engineered strong coupling between 2DEG modes and a Fabry-Pérot cavity was studied and showed that just a fractional absorption by 2DEG plasmons was observed in the transmission spectrum at 8 K.[8] Both the cavity and the grating were found applicable to control the coupling of the THz field and 2DEG plasmons.

The radiation power from 2DEG plasmonic devices was theoretically estimated to be around 2 mW.[5] However, in the experiments, only a little fraction of the predicted power was observed with a He-cooled THz detector.[11,15,16] Recently, a high power emission of up to 2 μW with a power conversion efficiency of 1.6×10^{-6} in the range of 0.5–4.0 THz at room temperature (RT) was reported in AlGaN/GaN structures with a sub-micrometer grating of ohmic contacts.[17] A substantially smaller power of THz radiation was reported by a submicrometer gate on AlGaN/GaN HEMT, demonstrating the spectral tunability of the emission peak by the gate voltage between 0.75 and 2.1 THz.[16,18] However, the THz emission spectrum was found broad due to the radiative decay of a non-coherent electron plasma. In addition, there were no experiments that investigated the ratio between the intensity of plasmonic THz emission and the background radiation of an electrically driven plasmonic channel.

In this work, the THz spectra of the electrically driven 2DEG plasmons were demonstrated in AlGaN/GaN structures. The critical temperature of the distinguishable radiation of the 2DEG plasmons was estimated to be approximately 250 K. An additive contribution of radiation from both gated and ungated plasmons in the lateral conductive channel was considered; however, only the fundamental mode of ungated 2DEG plasmons was experimentally observed radiating a peak power of up to 940 nW at an electric field of 450 V/cm. The THz spectra of electrically driven plasmons were

a)Author to whom correspondence should be addressed: irmantas.kasalynas@ftmc.lt.

measured by using a far-infrared Fourier transform spectrometer (FTS) and optimized front optics with a capability to perform measurements in a vacuum. Plasmon emission was observed at the linear slope of current-voltage (I/V) characteristic. It was limited by an excess heat of the plasmonic sample and the electroluminescence of impurities.

The plasmonic sample used in this study is shown in Fig. 1. The $Al_{0.23}Ga_{0.77}N$/AlN/GaN heterostructures were grown on a 430 μm thick sapphire substrate by using the MOVPE method (UNIPRESS wafer #TG2196). The characterization of the structures at RT revealed that the gated 2DEG density, mobility, and distance to the surface were $n_{2DEG} = 5 \times 10^{12}$ cm^{-2}, $\mu_{RT} = 1400$ cm^2/V s, and $d = 26$ nm, respectively.[19] The nominal value of 2DEG density in ungated regions was found from Hall measurements of ungated Van-der-Pauw structures, and it was about 9×10^{12} cm^{-2}. At a temperature of T = 77 K of liquid nitrogen (LN), the mobility of about $\mu_{LN} = 4170$ cm^2/V s was measured without noticeable carriers being froze-out, indicating a good localization of 2DEG by the AlN spacer.

The grating, consisting of metal stripes of $a = 0.35$ μm width and $P = 1.0$ μm period, was made on top of the AlGaN surface over the area of 2×2 mm^2 using an standard lift-off procedure with the electron-beam lithography definition of the pattern, development, and sputtering of Ti/Au with a thickness of 5/40 nm. Two ohmic contacts one at each side of the grating were fabricated by standard ultraviolet photolithography to provide an electric current flow through the 2DEG channel in direction parallel to the grating vector $k_g = 2\pi/P$.[20]

Pulse excitation of the plasmonic sample was implemented using the Source/Measurement unit (Keysight B2901A) to measure the electric current through the 2DEG channel in response to the applied voltage. Heating of the sample was minimized using a millisecond duration pulsed-excitation at a repetition rate (RR) of 12.5 Hz determined by the optimal performance of the THz detector (Golay cell). The THz emission spectra in the normal direction to the grating plane were measured by the FTS in the frequency range of 50–500 cm^{-1} defined by the 6 μm polyethylene beam-splitter (see details in Ref. 21). In order to exclude the interference effects from Fabry-Pérot oscillations, the spectral resolution of 6 cm^{-1} was chosen.

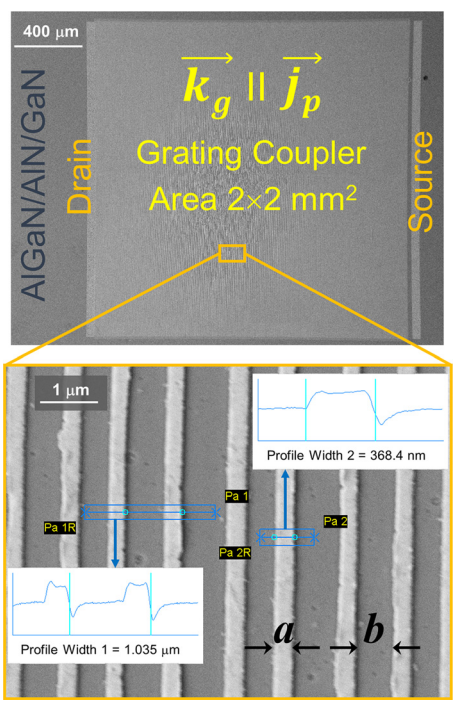

FIG. 1. Scanning electron microscopy (SEM) image of the plasmonic sample. Here, a is the width of grating-fingers, b the spacing between adjacent fingers, $P = a + b$ the period, $\vec{k}_g$ the grating vector oriented in parallel to the electric current $j_p || k_g$, and $k_g = \frac{2\pi}{P}$.

The spatial resolution of sample's radiation was obtained with a custom design of the collecting optics. A parabolic mirror of a numerical aperture of 0.45 was used to collect the THz radiation from the spot of 1.5 mm in diameter. The collimated radiation via an aperture of 25 mm was gathered into a solid angle of 0.18 srad.[20]

The sample was mounted on an optical holder of the LN cryostat equipped with the temperature sensor and the heater used to control the temperature in the range of 100–400 K. Three-axis-translation stage positioned the sample accurately on the optical axis of the FTS. The measurement zone on the plasmonic sample was precisely controlled within the footprint of the grating. The induced heat was extracted from the plasmonic sample via a sapphire substrate clamped on the cold finger of the cryostat. There were no metal-surfaces under the plasmonic sample in order to avoid interference effects from the back-reflection of electromagnetic waves. All the experiments were performed in a vacuum, minimizing the artifacts due to the THz absorption by water vapor.

The THz radiation power was measured with the calibrated Golay cell detector assuming that its response was independent of the frequency over the entire spectral range of interest. Thermally stimulated radiation from the SiC crystal placed instead of the plasmonic sample was used to calibrate the optical losses of the FTS.[20,21]

Gated and ungated 2DEG plasmon dispersion was modeled using the procedure described by Popov and coauthors.[7,22] The plasmonic sample was designed to generate the fundamental mode of gated and ungated 2DEG plasmons at frequencies 68 cm^{-1} and 166 cm^{-1}, respectively. To avoid the poor coupling efficiency of the gated plasmon radiation due to a short scattering length of a sub-micrometer gate, the second mode of gated plasmons was designed to match the fundamental mode of the ungated plasmons in order to increase the interaction between them in the channel.[7]

It was noticed that with the temperature increase from 300 K to 307 K, the polarized THz radiation was emitted from the plasmonic sample with an average optical power of about 4 μW. In such a case, a THz polarizer was used to confirm the polarization perpendicular to the grating lines. This radiation performance of a thermally stimulated plasmonic sample was comparable with the earlier reported results.[17]

The I/V characteristic of the plasmonic sample was measured at a cryostat temperature 110 K. The results are shown in Fig. 2. At an electric field below 100 V/cm, the conductance of the 2DEG channel was independent on the duty cycle (DU) of the applied voltage pulses. The sheet resistance was about 200 Ohm/sq, the same as measured at the low dc-bias conditions.

At higher electric field values, the decrease in the electrical conductance of the 2DEG channel was observed with

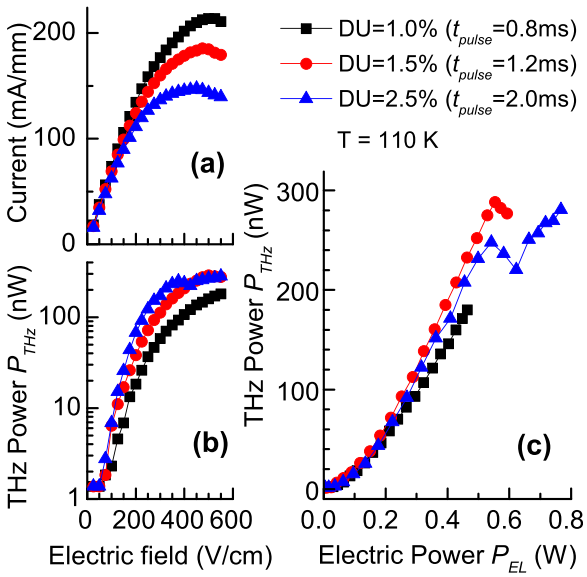

FIG. 2. Current density (a) and average emitted optical power (b) of the plasmonic sample dependence on the electric field; the P_{THz} dependence on the average electric power (c) supplied to the plasmonic sample at a temperature of 110 K. Measurements were performed using the voltage pulses of selected duration t_{pulse}. The average optical power was measured with the calibrated Golay cell detector.

the increase in DU. A saturation current was found to be limited by the electric field and DU values. The maximum current density of 220 mA/mm was obtained, which was not typical for the high electron mobility transistors.[19,23] The Joule heating of the sample was not possible to notice from the readings of the temperature sensor of the cryostat. However, the I/V performance clearly indicated the accumulation of an excess heat in the sample due to a limited convectional cooling and thermal conductance of the substrate. Thus, the plasmonic sample was driven in a linear I/V regime without a noticeable mobility dependence from the applied electric field.[24] Indeed, a higher current density of up to 20% was possible to obtain in the same setup but with a reduced pulse RR value to 1 Hz.

The average THz power radiated from the plasmonic sample at different pulse-biases is shown in Fig. 2(b). The THz radiation was measured within uncertainty of the experiment when the applied electric field exceeded the value of about 50–70 V/cm. In contrast, the THz power versus electric field dependence demonstrated a more intense THz emission at the higher DU values. The $P_{THz}(E)$ characteristic demonstrated a saturation behavior which was also more pronounced at the higher DU. The maximum average THz power emitted in a normal direction from the plasmonic sample was found to be approximately 300 nW for all the cases studied.

The average electric power supplied to the plasmonic sample (P_{EL}) was also measured. The $P_{THz}(P_{EL})$ dependence is shown in Fig. 2(c), revealing a nonlinear behaviour with an obvious peak at $P_{EL} \approx 0.55$ W. The peak value corresponded to the temperature of the plasma channel of about $T_{cr} \approx 240$ K, which was estimated from the measurements of the low-field-resistance vs temperature (data not shown). Moreover, the intensity of the THz emission was increased up to 80% of the RT value when the sample temperature was close to T_{cr}.

The emission of the plasmonic sample at $E = 300$ V/cm and DU = 5% was compared with the thermal radiation of the SiC crystal measured for calibration purposes. The results are shown in Fig. 3(a). The spectra of both sources were similar in the shape but different in the spectral intensity; the intensity of the plasmonic sample emission was up to two orders of magnitude smaller due to used electrical pulse excitation and operation at cryogenic temperature.

Figure 3(b) shows the emission spectra measured at the fixed electric field but at different DUs ranging from 5.0% to 0.5%. At DU = 1.0%, the THz radiation power was sufficient to exceed the noise level of the experiment, and the spectrum was found to be rich with distinctive features co-existing together with the 2DEG plasmon radiation. The emission spectrum at the 10 THz frequency can be divided into the red and blue spectral wings identified better by presenting data in the radiance scale and accounting spectral alterations induced by the used beam splitter.

The measured spectral radiant flux of the plasmonic sample is shown in Fig. 4. The thermal black-body (BB) like radiation of the plasmonic sample was distinguishable at the blue-wing spectrum at DU<5.0% and developed into a continuous spectrum at DU = 5.0% or larger. Thus, even when the sample was cooled down in the cryostat, the intensity of the thermal radiation was significantly contributing to the 2DEG plasmon radiation without a noticeable change in the cryostat temperature readings. A stop band observed at the 10 THz frequency was attributed to the simultaneous emission of different THz sources and to a nonuniform temperature of the plasmonic sample excited in a pulsed regime.

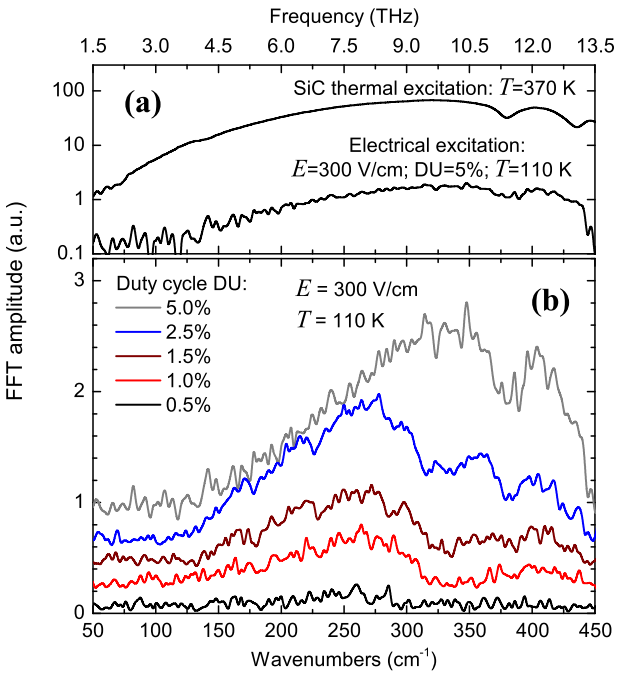

FIG. 3. (a) Emission of the plasmonic sample in comparison to the thermal radiation of the SiC crystal used for calibration purposes. Note that the vertical scale is logarithmic, and different regimes of the sample excitation were involved. (b) Emission spectra of the plasmonic sample driven electrically in a pulse regime at a temperature of 110 K under an electric field of $E = 300$ V/cm. The pulse durations of applied voltage was 0.4, 0.8, 1.2, 2.0, and 4.0 ms for each spectrum offset vertically by 0.2 a.u.

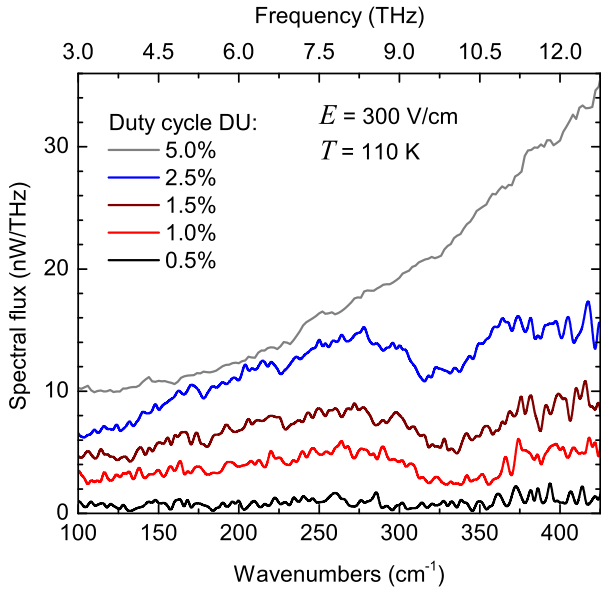

FIG. 4. Radiance of the plasmonic sample derived from the results shown in Fig. 3(b). Each of the spectrum was offset vertically by 2 nW/THz.

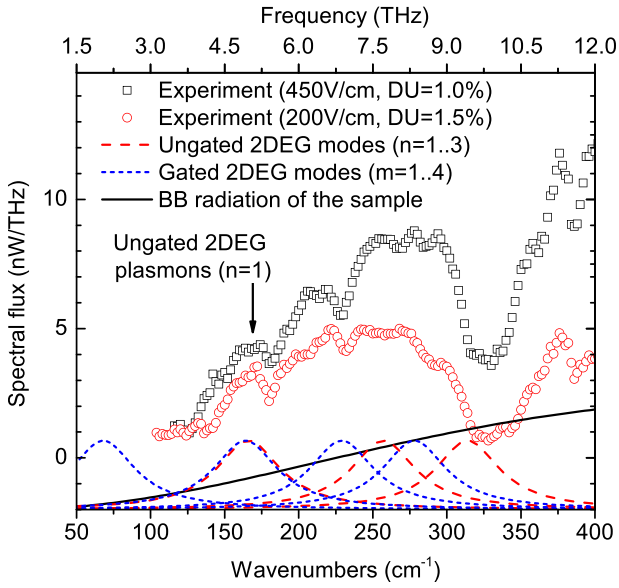

FIG. 5. Radiance of the plasmonic sample under electric fields of 200 V/cm and 450 V/cm. The ungated and gated modes of 2DEG plasmons calculated up to the fifth order are shown as dashed (red) and dotted (blue) lines, respectively. The thermal BB radiation is shown by the solid line (black). The impurities' luminescence band spans from 180 cm^{-1} to 210 cm^{-1} with the hot electron transitions from the conduction band to the ground states of O donors contributing to the broad peak centered at 270 cm^{-1} wavenumbers as described in Ref. 25.

In the red-wing spectral region, the first peak at the 166 cm^{-1} frequency was attributed to the fundamental mode of the ungated 2DEG plasmons. The P_{THz} saturation at an electric field larger than 300 V/cm (Fig. 2(b)) was ascribed to a contribution from an excess heat accumulation which led to the attenuation of radiation from the 2DEG plasmons. Thus, the THz spectrum was found to be intermixed with the spectrum of thermal BB radiation and the electroluminescence of impurities[25] and was investigated separately (see discussion below).

Finally, the THz radiation spectra were measured at different electric field strengths (Fig. 5). The calculated spectra of the gated and ungated plasmon modes and the thermal BB radiation are also presented. The peak emission of the 2DEG plasmons was found to be weakly dependent on the applied electric field. For example, the change from 200 V/cm to 450 V/cm resulted in a small amplitude increase by ~20%.

Signatures of higher modes' emission from 2DEG plasmons were also measured. The emission was found to be significantly contaminated by intense electroluminescence from Si and O impurities located in the close proximity of the 2DEG channel.[26,27] Apparently, the electroluminescence was contributing to emission at significantly lower electric fields and at higher temperatures as compared to earlier observations,[25] most probably, due to the quality of the fabricated ohmic contacts. In this study, the oxygen was the main source of impurities' emission present in the MOVPE grown heterostructure layers. The residual oxygen doping can be reduced from 10^{17} cm^{-3} up to 5×10^{15} cm^{-3}, expecting the corresponding attenuation of the unwanted electroluminescence signal.

The THz emission spectra of electrically driven plasmons were studied at longer wavelengths by the replacement of a 6 μm beam splitter by 12 μm and 50 μm thick ones that improved the FTS sensitivity at frequencies down to 20 cm^{-1}. Accordingly, the emission spectrum was modified. However, the peak of the gated 2DEG plasma radiation of the fundamental mode was still undistinguishable. The result was expected since the theory predicted a weak coupling efficiency of the gated plasmons.[7]

The gated and ungated plasmons' radiation efficiency was theoretically analysed in Refs. 6 and 7, showing a weak relationship between the radiation efficiency and sample's temperature. A higher radiation efficiency is expected at low temperatures due to a decrease in the damping constant and, at the same time, an increase in the electrons' momentum relaxation time τ_m, which allows us to meet the condition of efficient emission $\omega_p \tau_m > 1$ at lower frequencies.

The linewidth of the ungated plasmons was found to be $\Delta f_c = 52.5\,cm^{-1}$ (1.56 THz) by fitting the peak at $f_c = 166\,cm^{-1}$ (5.0 THz) with the Lorentzian function (data shown in Fig. 5). The value of the quality factor $Q_c = f_c/\Delta f_c = 3.2$ was found to be similar to that reported for an electrically driven plasmonic device.[9]

The absolute THz power of the ungated 2DEG plasmon radiation in a fundamental mode was estimated from data shown in Fig. 5. The average THz power was found to be about 6.3 nW and 9.4 nW at the electric fields of 200 V/cm and 450 V/cm or in terms of the average electric powers of 0.15 W and 0.38 W, respectively. Accounting for the DU scaling, the peak THz power value was about 420 nW and 940 nW, respectively. The energy conversion efficiency of the ungated 2DEG plasmon radiation was 42×10^{-9} and 25×10^{-9}, respectively. It is noteworthy that the THz power of the background radiation was not excluded from the results. On the other hand, the efficiency of the thermal BB radiation was estimated to reach 3.6×10^{-7} at P_{EL}=0.77 W (Fig. 2(c)). Therefore, the issue of an excess heat of the plasmonic sample should be properly addressed in future studies aiming for practical applications. An improved heat-sink design and development of plasmonic samples on SiC or

native GaN substrates with higher thermal conductance[23] would benefit the performance of electrically driven plasmonic THz emitters. The detailed measurement of these quantities should be a focus of future studies.

In conclusion, the electrically driven THz radiation of 2DEG plasmons in AlGaN/AlN/GaN has been observed at a temperature of 110 K. The spectrum of 2DEG plasmons was found to be enriched with the signatures from the heated sample radiation and impurities' electroluminescence. In the 2DEG plasmon excitation regime, the peak THz power was obtained up to 940 nW with the electrical-to-optical conversion efficiency of up to 42×10^{-9} depending on the strength of the applied electric field. The optical vs electrical power characterisation revealed that only a limited electrical power can be used for the efficient 2DEG plasmon excitation. The results showed an unexplored potential of a electrically driven plasmonic devices as compact and reliable THz sources.

This work was supported by the Research Council of Lithuania (Grant No. LAT 04/2016), and the activities at Warsaw were supported by the National Science Centre of Poland (Grant No. DEC-2013/10/M/ST3/00705).

[1]S. J. Allen, D. C. Tsui, and R. A. Logan, Phys. Rev. Lett. **38**, 980 (1977).
[2]J. Wu, A. S. Mayorov, C. D. Wood, D. Mistry, L. Li, W. Muchenje, M. C. Rosamond, L. Chen, E. H. Linfield, A. G. Davies, and J. E. Cunningham, Sci. Rep. **5**, 15420 (2015).
[3]D. Olego, A. Pinczuk, A. C. Gossard, and W. Wiegmann, Phys. Rev. B **25**, 7867 (1982).
[4]A. V. Muravjov, D. B. Veksler, V. V. Popov, O. V. Polischuk, N. Pala, X. Hu, R. Gaska, H. Saxena, R. E. Peale, and M. S. Shur, Appl. Phys. Lett. **96**, 42105 (2010).
[5]M. Dyakonov and M. Shur, Phys. Rev. Lett. **71**, 2465 (1993).
[6]S. A. Mikhailov, Phys. Rev. B **58**, 1517 (1998).
[7]V. V. Popov, O. V. Polischuk, and M. S. Shur, J. Appl. Phys. **98**, 33510 (2005).
[8]Y. Huang, H. Qin, B. Zhang, J. Wu, G. Zhou, and B. Jin, Appl. Phys. Lett. **102**, 253106 (2013).
[9]S. Boubanga-Tombet, F. Teppe, J. Torres, A. El Moutaouakil, D. Coquillat, N. Dyakonova, C. Consejo, P. Arcade, P. Nouvel, H. Marinchio, T. Laurent, C. Palermo, A. Penarier, T. Otsuji, L. Varani, and W. Knap, Appl. Phys. Lett. **97**, 262108 (2010).
[10]G. C. Dyer, G. R. Aizin, S. Preu, N. Q. Vinh, S. J. Allen, J. L. Reno, and E. A. Shaner, Phys. Rev. Lett. **109**, 126803 (2012).
[11]K. Hirakawa, K. Yamanaka, M. Grayson, and D. C. Tsui, Appl. Phys. Lett. **67**, 2326 (1995).
[12]G. C. Dyer, G. R. Aizin, S. J. Allen, A. D. Grine, D. Bethke, J. L. Reno, and E. A. Shaner, Nat. Photonics **7**, 925 (2013).
[13]M. S. Shur and V. Ryzhii, Int. J. High Speed Electron. Syst. **13**, 575 (2003).
[14]M. I. Dyakonov and M. S. Shur, IEEE Trans. Electron Devices **43**, 1640 (1996).
[15]D. Tsui, E. Gornik, and R. A. Logan, Solid State Commun. **35**, 875 (1980).
[16]A. El Fatimy, N. Dyakonova, Y. Meziani, T. Otsuji, W. Knap, S. Vandenbrouk, K. Madjour, D. Théron, C. Gaquiere, M. A. Poisson, S. Delage, P. Prystawko, and C. Skierbiszewski, J. Appl. Phys. **107**, 24504 (2010).
[17]T. Onishi, T. Tanigawa, and S. Takigawa, Appl. Phys. Lett. **97**, 92117 (2010).
[18]W. Knap, S. Nadar, H. Videlier, S. Boubanga-Tombet, D. Coquillat, N. Dyakonova, F. Teppe, K. Karpierz, J. Łusakowski, M. Sakowicz, I. Kasalynas, D. Seliuta, G. Valusis, T. Otsuji, Y. Meziani, A. El Fatimy, S. Vandenbrouk, K. Madjour, D. Théron, and C. Gaquière, J. Infrared, Millimeter, Terahertz Waves **32**, 618 (2011).
[19]V. Jakštas, I. Kašalynas, I. Šimkienė, V. Strazdienė, P. Prystawko, and M. Leszczynski, Lith. J. Phys. **54**, 227 (2014).
[20]I. Kašalynas, R. Venckevičius, J. Laužadis, V. Jakštas, E. Širmulis, K. Požela, and G. Valušis, J. Phys. Conf. Ser. **647**, 12005 (2015).
[21]K. Požela, E. Širmulis, I. Kašalynas, A. Šilėnas, J. Požela, and V. Jucienė, Appl. Phys. Lett. **105**, 91601 (2014).
[22]V. V Popov, J. Infrared, Millimeter, Terahertz Waves **32**, 1178 (2011).
[23]P. Kruszewski, P. Prystawko, I. Kasalynas, A. Nowakowska-Siwinska, M. Krysko, J. Plesiewicz, J. Smalc-Koziorowska, R. Dwilinski, M. Zajac, R. Kucharski, and M. Leszczynski, Semicond. Sci. Technol. **29**, 75004 (2014).
[24]V. A. Shalygin, L. E. Vorobjev, D. A. Firsov, A. N. Sofronov, G. A. Melentyev, W. V. Lundin, A. E. Nikolaev, A. V. Sakharov, and A. F. Tsatsulnikov, J. Appl. Phys. **109**, 73108 (2011).
[25]V. A. Shalygin, L. E. Vorobjev, D. A. Firsov, V. Y. Panevin, A. N. Sofronov, G. A. Melentyev, A. V. Antonov, V. I. Gavrilenko, A. V. Andrianov, A. O. Zakharyin, S. Suihkonen, P. T. Törma, M. Ali, and H. Lipsanen, J. Appl. Phys. **106**, 123523 (2009).
[26]W. J. Moore, J. A. Freitas, G. C. B. Braga, R. J. Molnar, S. K. Lee, K. Y. Lee, and I. J. Song, Appl. Phys. Lett. **79**, 2570 (2001).
[27]H. Wang and A.-B. Chen, J. Appl. Phys. **87**, 7859 (2000).